Zinc(II) halide and copper(II) bromide complexes with caffeine: structures, physicochemical properties, and biological activity*

N. S. Rukk,[a]★ L. G. Kuzmina,[b] G. A. Davydova,[c] G. A. Buzanov,[b] S. K. Belus,[d] E. I. Kozhukhova,[d] V. M. Retivov,[d] T. V. Ivanova,[a] V. N. Krasnoperova,[a] and B. M. Bolotin[d]

[a]*MIREA — Russian Technological University, M. V. Lomonosov Institute of Fine Chemical Technologies, 86 prosp. Vernadskogo, 119571 Moscow, Russian Federation. Fax: +7 (495) 434 9287. E-mail: roukkn@inbox.ru*

[b]*N. S. Kurnakov Institute of General and Inorganic Chemistry, Russian Academy of Sciences, 31 Leninsky prosp., 119991 Moscow, Russian Federation. Fax: +7 (495) 954 1279*

[c]*Institute of Theoretical and Experimental Biophysics, Russian Academy of Sciences, 3 Institutskaya ul., 142290 Pushchino, Moscow region, Russian Federation. Fax: +7 (496 7) 33 0553*

[d]*Institute of Chemical Reagents and High Purity Chemical Substances of National Research Center "Kurchatov Institute", 3 Bogorodskii val, 107076 Moscow, Russian Federation. Fax: +7 (495) 963 7071*

This study provides a comparative characterization of the structural parameters and cytotoxicity of zinc halide and copper(II) bromide complexes with caffeine (caf) of the composition $[Zn(caf)(H_2O)X_2]$ (X = Cl, Br, I) and $[Cu(caf)_2Br_2]$ (**1**). The cytotoxicity of the complexes is dose-dependent in all cell lines. The concentrations of the complexes, at which they are more cytotoxic against cancer cells (MCF-7) than against stem cells (DPSC), were determined. The synthesized complexes exhibited synergism of cytotoxicity.

Key words: zinc(II) halides, copper(II) bromide, caffeine, square-planar structure, molecular complex, cytotoxicity.

According to the World Health Organization (WHO), cancer is the second leading cause of death (after cardiovascular diseases) worldwide, accounting for about 13% of all deaths.[1] According to estimates from the International Agency for Research on Cancer (IARC), in 2018 there were 17 million new cancer cases and 9.5 million cancer deaths worldwide, *i.e.*, 26,000 deaths a day.** The continuing global demographic and epidemiologic transitions signal an ever-increasing cancer burden, and cancer rates expected to hit 20 million new cases per year by 2025.[1] Hence, a challenging problem is to develop new anticancer agents equally or more effective than platinum-based drugs, which exhibit toxicity, drug resistance, and other adverse side effects.[2—5]

A major intracellular target of anticancer agents based on transition metal complexes is deoxyribonucleic acid (DNA). These drugs cause various DNA damages, blockage of cell division, and cell death. The covalent interaction of small metal complexes with the DNA double helix *via* intercalation into a DNA molecule followed by the binding in the DNA major and minor grooves is an essential binding mode resulting in the irreversible degradation and cell destruction.[3] Cyclin-dependent kinases regulating the cell cycle serve as an alternative target.[6]

Copper and zinc are essential elements for living organisms, as they are involved in fundamental life processes and can exhibit anticancer activity.[7] Copper-containing compounds are known to have selective cytotoxicity against cancer cells due to a low oxygen content in regions surrounding malignant tumors, resulting in the reduction of Cu^{II} to Cu^{I}, the cleavage of double-stranded DNA, and the formation of reactive oxygen species (ROS).[8,9] Metals capable of existing in different oxidation states (Cu^{II}, Mn^{II}, Mn^{III}) are mainly involved in redox processes, whereas Zn^{II} and Ni^{II} participate in radical-type reactions.[10] However, mono- and binuclear zinc halide complexes with ligands synthesized by the Mannich reaction[10] exhibited anticancer activity against Jurkat T-lymphocyte

* Based on the materials of the XXI Mendeleev Congress on General and Applied Chemistry (September 9—13, 2019, St. Petersburg, Russia).

** https://www.cancer.org/research/cancer-facts-statistics/global.html.

Published in Russian in *Izvestiya Akademii Nauk. Seriya Khimicheskaya,* No. 7, pp. 1394—1400, July, 2020.

leukemia cells; at concentrations of 100 μg mL^{-1}, the cytotoxicity of the halide complexes changes in the order $Cl^- > Br^- > I^-$ for both types of compounds (the viability was 44.77, 48.08, 59.88%, and 37.98, 38.97, 40.7%, respectively). A similar phenomenon was observed for zinc halide complexes with caffeine.[11] Reactive oxygen species measurements demonstrated that the above-mentioned mono- and binuclear zinc halide complexes represent a rare example of an important role of zinc in the ROS generation. This is due to the fact that during oxidative stress, glutathione production becomes insufficient in neutralizing ROS. It was also shown that the excess production of ROS leads to oxidative DNA damage and apoptosis.[10]

Caffeine (1,3,7-trimethyl-1*H*-purine-2,6-(3*H*,7*H*)-dione, caf) and its derivatives, in particular proxyfeine (8-oxycaffeine γ-dimethylaminopropyl ether) and the radiosensitizing agent xanthobin (8-bromocaffeine), can be used in the development of drugs and in combination therapies of brain tumors due to their ability to cross the blood-brain barrier.[12,13] Therefore, these compounds are promising for the preparation of drugs for cancer therapy, including the therapy of radio- and chemo-resistant neuroblastoma, in particular brain tumors. It is worth noting that these agents can be used in patients at high risk for brain metastases.[12]

Biologically active platinum(II),[14] gold(III),[15] and silver(I)[16] complexes with caffeine and its derivatives were described in the literature. For instance, silver(I) acetate complexes with caffeine, theophylline, and theobromine derivatives were evaluated for antiproliferative activity in relation to cisplatin against eight cancer cell lines: A375 (malignant melanoma), HCT116 (human colorectal adenocarcinoma), HT-29 (colon adenocarcinoma), LN229, U-87 MG, U-251 (glioblastomas), Panc-1 (pancreatic carcinoma), and SiHa (cervical cancer).[16] These complexes exhibited moderate cytotoxicity, with half-maximal inhibitory concentrations (IC_{50}) in a micromolar range. The bis-carbene complex [Au(caffein-2-ylidene)$_2$][BF_4] is known to be selective toward human ovarian cancer cell lines and is non-toxic to normal cells,[17] whereas the caffeine derivative of the square-planar rhodium(I) complex [Rh(I)Cl(COD)(NHC)] with *N*-heterocyclic carbene (NHC) and 1,5-cyclooctadiene (COD) combines cytotoxicity against various tumor cell lines and also antimetastatic and antiangiogenic effects.[18]

The copper(II) chloride complex with caffeine [Cu(caf)-(H_2O)Cl_2] was described;[19] however, its biological activity was not evaluated. Data on copper bromide complexes with caffeine are absent in the literature. Therefore, the goal of this work is to synthesize and characterize the caffeine derivative of copper bromide and compare its biological activity with that of the zinc halide complexes with caffeine studied earlier.[11,20]

The complex [Cu(caf)$_2$$Br_2$] (**1**) was prepared in an aqueous solution from copper(II) bromide and caffeine, taken in the molar ratio $CuBr_2$: caf = 1 : (0.8—2), followed by heating until the solvent was almost completely removed and dark-brown crystals were formed (Scheme 1).

Scheme 1

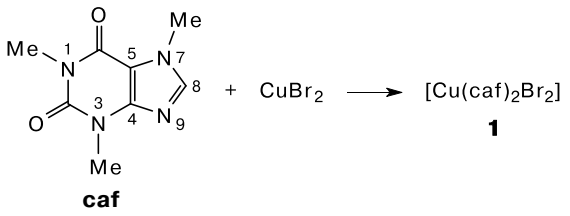

Compound **1** was identified by chemical and elemental analyses, powder X-ray diffraction, single-crystal X-ray diffraction, IR and ^{1}H NMR spectroscopy, and mass spectrometry. Homogeneity of the samples was confirmed by a comparison of the X-ray diffraction patterns of the starting compounds with the experimental X-ray diffraction pattern and the simulated pattern of compound **1** (Fig. 1). Therefore, compound **1** was isolated in individual state without impurities of the reagents or other compounds. The simulated X-ray diffraction pattern based on the single-crystal X-ray diffraction data coincides with the experimental pattern. Hence, the single-crystal structure is representative for the bulk sample.

The mass spectra are indicative of the formation of the complex species [Cu(caf)$_2$Br]$^+$ (m/z 532.01$^+$), [Cu(caf)$_2$]$^+$ (m/z 451.14$^+$) and other fragments, including caffeine clusters.

Complex **1** crystallizes in the monoclinic crystal system (space group $P2_1/n$; $Z = 4$; $a = 18.4484(5)$ Å, $b = 6.4101(2)$ Å, $c = 19.0059(5)$ Å, $\beta = 111.2870(10)°$) and is characterized by square-planar geometry (two Br^- anions and two nitrogen atoms N(9) of caffeine molecules are in *trans* positions) (Fig. 2, Table 1). The unit cell parameters calculated from the single-crystal X-ray diffraction data are in good agreement with those calculated from the powder X-ray diffraction data. Selected bond lengths and bond angles are given in Table 2. A comparison of the M—X and M—N bond lengths shows that the Cu—N bond length of complex **1** is shorter (1.9692—1.9784 Å) than those of the zinc compounds: the Zn—N distances vary from 2.068 (X = Cl) to 2.074 (X = Br) and 2.053 Å (X = I), while the M—X bond length has an intermediate value for the copper derivative (2.4098—2.4211 Å for M = Cu; 2.206—2.558 Å for M = Zn). The average distance between the bound bromide ion and the *cis*-nitrogen atom of the coordinated caffeine molecule in **1** is 3.121 Å and is similar to the N(1)—O(3) distance in [Zn(caf)(H_2O)Br_2][11] (3.124 Å).

The coordination of caffeine is confirmed by IR spectroscopy. Thus, the absorption band at 1597 cm^{-1} assigned

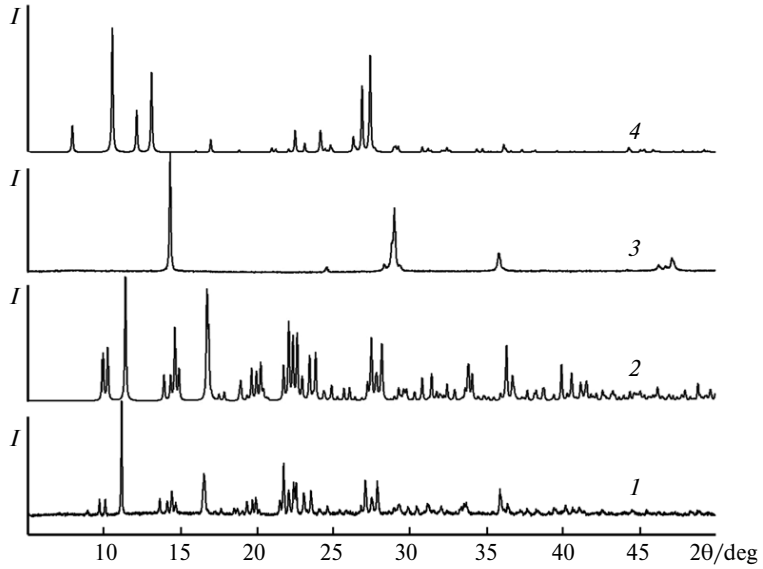

Fig. 1. Experimental powder X-ray diffraction pattern of complex **1** (*1*), the simulated diffraction pattern of **1** (*2*) based on single-crystal X-ray diffraction data, and the powder diffraction patterns of the starting compounds $CuBr_2$ (*3*) and caf • H_2O (*4*).

to bending vibrations δ(NCN) of caffeine is shifted to longer wavelengths upon coordination of the ligand through the nitrogen atom N(9) (1554 cm^{-1}, ν(Cu—N) + + δ(NCN)). The coordination of bromide ions is confirmed by the presence of absorption bands at 200—300 cm^{-1}.

Cytotoxicity was evaluated using the MTT assay[20—22] in postnatal human dental pulp stem cells (DPSC)[20] and the MCF-7 cell line (breast cancer cell line). The statistical data processing was performed using the Origin program, the error was taken as the root-mean-square

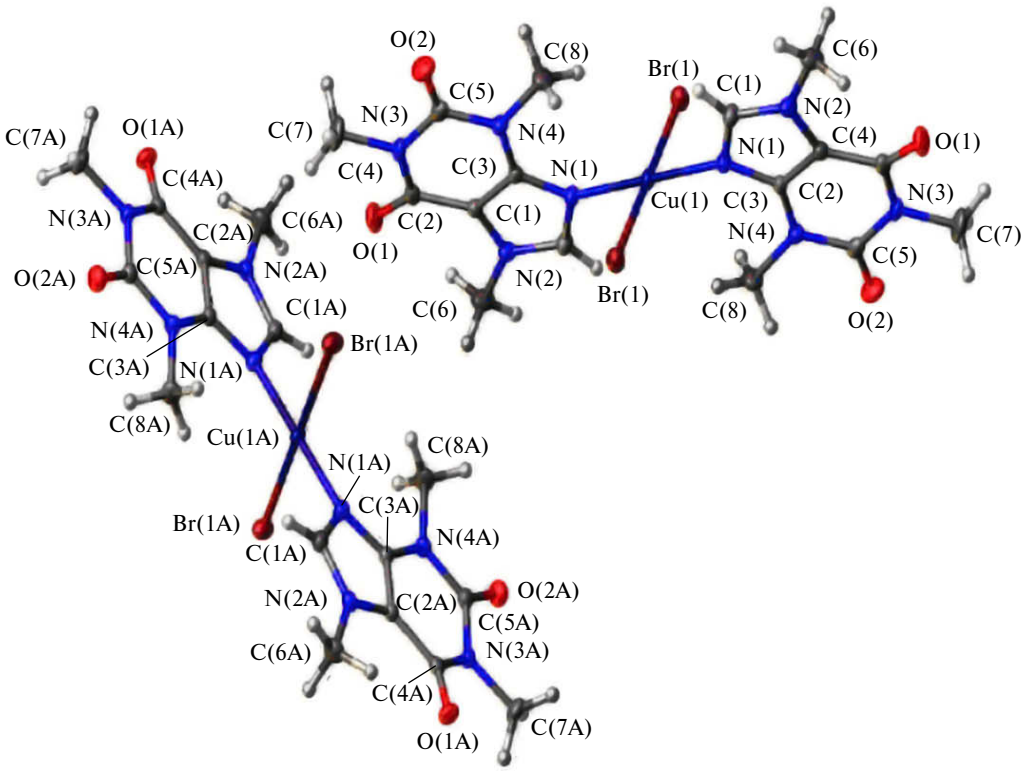

Fig. 2. Structure of the complex $[Cu(caf)_2Br_2]$ (**1**).

Table 1. X-ray diffraction data collection and refinement statistics for the complex $[Cu(caf)_2Br_2]$ (**1**)

Parameter	Value
Compound	$[Cu(C_8H_{10}N_4O_2)_2Br_2]$
Empirical formula	$C_{16}H_{20}Br_2CuN_8O_4$
Molecular weight	611.76
Radiation	Mo-Kα
λ/Å	0.71073
T/K	150
Crystal system	Monoclinic
Space group	$P2_1/n$
Z	4
a/Å	18.4484(5)
b/Å	6.4101(2)
c/Å	19.0059(5)
α/deg	90.00
β/deg	111.287(1)
γ/deg	90.00
V/Å^3	2094.22(10)
d_{calc}/g cm^{-3}	1.940
μ/mm^{-1}	4.902
F(000)	1212
Scan range, θ/deg	2.37—28.24
Index ranges *hkl*	$-24 \leqslant h \leqslant 24$; $-8 \leqslant k \leqslant 8$; $-25 \leqslant l \leqslant 25$
Crystal size/mm (brown block)	0.46×0.36×0.08
Number of reflections	
measured	5178
with $I > 2\sigma(I)$	4322
Number of refined parameters	289
GOOF	1.035
R_1	0.0223
wR_2 (for $I > 2\sigma(I)$)	0.0502
R_1	0.0302
wR_2 (based on all data)	0.0527

Table 2. Selected bond lengths (*d*) and bond angles (ω) of $[Cu(caf)_2Br_2]$

Parameter	Value
Bond	*d*/Å
Cu(1)—Br(1)	2.4098(2)
Cu(1)—N(1)	1.9784(18)
Cu(2)—Br(1)	2.4211(2)
Cu(2)—N(1)	1.9692(18)
Angle	ω/deg
Br(1)—Cu(1)—Br(1)	179.999(2)
N(1)—Cu(1)—N(1)	180.0
N(1)—Cu(1)—Br(1)	89.26(6)
N(1)—Cu(2)—Br(1)	88.77(6)

deviation from the mean, and the statistically significant difference was determined using the Mann—Whitney U test at $p < 0.01$.

Changes in the biological action upon complexation can be analyzed based on the data on cytotoxicity of the compounds and the corresponding stoichiometric mixtures against postnatal human dental pulp stem cells (DPSC) and the MCF-7 cell line (Tables 3 and 4, respectively). Cytotoxicity of the compounds is dose-dependent (Fig. 3) in both cell lines. The highest cytotoxicity was found at concentrations of $5 \cdot 10^{-5}$—$1 \cdot 10^{-4}$ mol L^{-1} in the MCF-7 cell line (compared to DPSC). At these concentrations, the complex is more toxic than the mixture of the initial components and the conventional doxorubicin (dox, $C_{27}H_{29}NO_{11}$) served as the standard (see Tables 3 and 4). Besides, significant differences ($p < 0.01$) from the control were found according to the Mann—Whitney U test in the MCF-7 cell line at concentrations of $5 \cdot 10^{-5}$—

Table 3. Cytotoxicity of the studied compounds and mixtures against primary DPSC cells

Compound	DPSC viability (%)* at *C*/mol L^{-1}			
	$1 \cdot 10^{-6}$	$1 \cdot 10^{-5}$	$5 \cdot 10^{-4}$	$1 \cdot 10^{-4}$
$[Zn(caf)(H_2O)Cl_2]$	62.43±18.67	79.62±13.83	53.05±16.5	35.64±8.52
$[Zn(caf)(H_2O)I_2]$	113.97±13.11	88.96±12.62	37.98±5.06	27.03±8.16
$[Zn(caf)(H_2O)Br_2]$	90.64±14.10	85.97±8.31	74.35±12.04	59.23±7.06
$[Cu(caf)_2Br_2]$	85.81±10.03	93.71±10.57	67.84±7.13	54.29±13.72
$ZnCl_2$ + caf	90.92±8.84	109.63±10.75	64.816±3.18	44.96±3.08
ZnI_2 + caf	92.42±2.71	100.72±14.93	57.96±8.40	44.75±5.33
$ZnBr_2$ + caf	109.63±20.31	77.73±24.88	72.02±5.11	54.49±12.10
$CuBr_2$ + caf	98.93±5.27	96.62±7.41	76.30±7.89	62.22±9.71
$ZnCl_2$	87.14±9.35	66.68±9.32	33.99±4.81	23.29±7.96
ZnI_2	74.19±9.48	69.27±34.63	35.13±11.54	35.01±6.33
$ZnBr_2$	89.27±4.95	78.51±16.73	71.77±7.98	62.37±5.82
$CuBr_2$	106.06±6.23	85.149±8.97	77.29±10.84	65.75±7.27
dox	101.59±6.84	79.09±5.63	64.87±12.68	58.79±10.92
caf	91.08±11.34	96.19±10.59	88.15±17.49	91.81±13.24

* Relative to the control.

Table 4. Cytotoxicity of the studied compounds and mixtures against the MCF-7 cell line

Compound	MCF-7 cell line viability (%)* at C/mol L^{-1}			
	$1 \cdot 10^{-6}$	$1 \cdot 10^{-5}$	$5 \cdot 10^{-4}$	$1 \cdot 10^{-4}$
$[Zn(caf)(H_2O)Cl_2]$	59.77±12.63	58.46±10.75	61.91±15.98	24.68±1.57
$[Zn(H_2O)(caf)I_2]$	108.41±12.73	112.48±7.46	54.76±10.64	29.09±4.09
$[Zn(caf)(H_2O)Br_2]$	84.80±12.25	82.16±15.35	15.70±5.58	16.78±6.08
$[Cu(caf)_2Br_2]$	87.49±9.99	78.08±12.67	56.31±5.02	10.87±1.77
$ZnCl_2$ + caf	101.10±14.58	91.10±10.74	86.23±8.38	65.16±8.043
ZnI_2 + caf	102.37±9.56	91.38±6.96	81.52±7.22	69.31±7.73
$ZnBr_2$ + caf	103.49±12.29	101.20±8.35	89.39±8.75	77.35±12.41
$CuBr_2$ + caf	92.14±9.64	87.37±12.52	82.99±10.78	73.22±11.22
$ZnCl_2$	98.87±9.63	92.28±11.29	47.11±6.41	28.45±6.33
ZnI_2	85.80±12.63	85.59±14.88	67.85±12.47	58.83±12.13
$ZnBr_2$	62.65±2.80	59.21±2.60	28.44±2.49	17.87±5.17
$CuBr_2$	103.06±10.24	91.34±11.33	75.27±10.69	31.62±5.21
dox	90.86±6.75	81.73±9.23	68.97±7.55	39.76±5.09
caf	82.52±16.89	108.49±11.18	82.58±15.91	74.10±14.43

* Relative to the control.

$1 \cdot 10^{-4}$ mol L^{-1} for all the complexes compared to stoichiometric mixtures.

Cytotoxicity of $[Cu(caf)_2Br_2]$ compared to the complexes $[Zn(caf)(H_2O)X_2]$ (X = Cl, Br, I) studied previously is more pronounced against the MCF-7 cell line (as compared to DPSC, Fig. 3) at a concentration of $1 \cdot 10^{-4}$ mol L^{-1}. Apparently, this is due to the planar structure of complex **1**, which facilitates its intercalation into DNA and causes DNA damage.[3] At this concentration, the cytotoxic effects of the zinc and copper bromide complexes are insignificantly different (within experimental error) apparently due to the nearly equal mutual distance between the ligands in *cis* positions of these complexes, which is close to the distance between adjacent base pairs along the DNA helix.

According to the Mann—Whitney U test ($p < 0.01$), significant differences in cytotoxicity against human dental pulp stem cells (DPSC) were found between $[Zn(caf)(H_2O)X_2]$ (X = Cl, I) and the corresponding stoichiometric mixtures, which is indicative of an increase in cytotoxicity upon complexation apparently as a result of the ROS generation leading to oxidative DNA damage.[10] The absence (the Mann—Whitney U test, $p < 0.01$) of significant differences in cytotoxicity against DPSC between the complexes $[Zn(caf)(H_2O)Br_2]$ and $[Cu(caf)_2Br_2]$ and their stoichiometric mixtures at concentrations of $5 \cdot 10^{-5}$—$1 \cdot 10^{-4}$ mol L^{-1} is apparently attributed to the fact that hypobromous acid (HOBr) is formed as the reactive intermediate in the presence of bromide ions, as opposed to

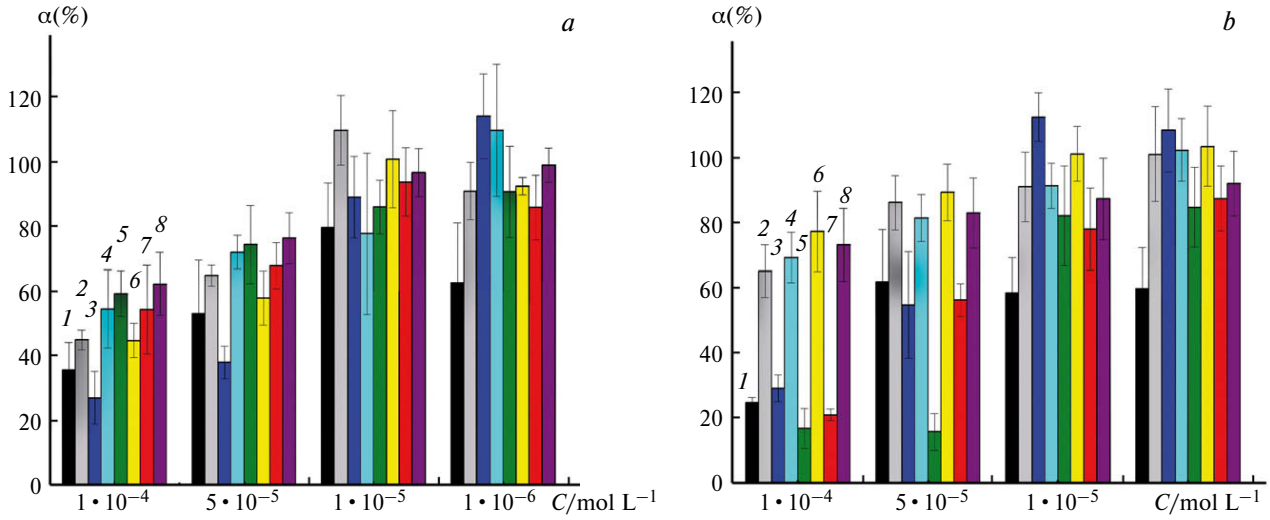

Fig. 3. Comparison of cytotoxicity of the complexes and mixtures of the starting compounds against the DPSC (*a*) and MCF-7 (*b*) cell lines: $[Zn(caf)(H_2O)Cl_2]$ (*1*), $ZnCl_2$ + caf (*2*), $[Zn(caf)(H_2O)I_2]$ (*3*), ZnI_2 + caf (*4*), $[Zn(caf)(H_2O)Br_2]$ (*5*), $ZnBr_2$ + caf (*6*), $[Cu(caf)_2Br_2]$ (*7*), $CuBr_2$ + caf (*8*); α is the cell viability (% of the control).

chloride and iodide ions. This acid is taken up by cultured cells and is incorporated into genomic DNA as 5-bromodeoxyuridine.[23]

In conclusion, we synthesized and identified a complex of the composition $[Cu(caf)_2Br_2]$ (**1**), determined its structure, and evaluated cytotoxicity against different cell lines. The complex was shown to have a molecular structure. Two bromide ions and two nitrogen atoms N(9) of caffeine molecules in mutually *trans* positions form a square-planar environment of the central copper(II) atom. The dose-dependent change in cytotoxicity was observed in all cell lines. Additional *in vivo* and *in vitro* studies are required for a more detailed characterization of biological activity.

Experimental

The compounds $[Zn(caf)(H_2O)X_2]$ (X = Cl, Br, I) were synthesized by a procedure described previously.[11,20] Elemental analysis was performed on a EuroVector EuroEA 3000 CHNS elemental analyzer (EuroVector s.p.a., Italy). The zinc and copper contents were determined by complexometric titration using Trilon; the bromide content was determined by the gravimetric method.[11,20] The IR spectra were recorded on a Bruker VERTEX 70 Fourier-transform infrared spectrometer in the region of 350—4000 cm^{-1} as KBr pellets and in the region of 30—680 cm^{-1} as Nujol mulls. Electrospray ionization mass spectra (ESI-MS) were obtained on an AmaZon Bruker Daltonik GmbH mass spectrometer (acquired over the mass range m/z = 70—2200) in positive and negative ion modes in a H_2O—MeCN solvent mixture (1 : 1). The ^1H NMR spectra were recorded on a Bruker Avance III NanoBay spectrometer (300.28 MHz, 25 °C, D_2O as the solvent, calibration using residual signals of HDO (δ 4.71)). Powder X-ray diffraction (XRD) patterns were measured on a Bruker D8 Advance X-ray diffractometer equipped with a LYNXEYE detector (Cu-Kα radiation, Ni filter, reflection geometry, 2θ angle range 5—80°, step size 0.01132°). Single-crystal X-ray diffraction data were collected on a CCD SMART APEX-II diffractometer (graphite monochromator, Mo-*K*α radiation, ω-scanning technique, 150 K). The X-ray diffraction data were processed using the SAINT program.[24] An absorption correction was applied with the SADABS program. The crystal structure was solved by direct methods and refined based on F^2 by the full-matrix least-squares method with anisotropic displacement parameters for nonhydrogen atoms. The hydrogen atoms were positioned geometrically and refined by the least-squares method using a riding model. All calculations were carried out with the Olex-2 software[25] and SHELXTL-Plus program package.[26] Principal crystallographic parameters are given in Table 1. The structural data were deposited with the Cambridge Crystallographic Data Centre (CCDC 1953834) and are available, free of charge, at http://www.ccdc.cam.ac.uk. The crystal structure visualization was performed using the MERCURY program.[27]

Dibromodi(caffeine)copper, $[Cu(caf)_2Br_2]$ (**1**), was synthesized in an aqueous solution (50 mL) from copper(II) bromide (0.75 g) and caffeine (0.51 g) pre-recrystallized from water, taken in the molar ratio $CuBr_2$: caf = 1 : 0.8, followed by heating until the solvent was almost completely removed and dark-brown crystals appeared. The yield was 0.66 g (82%). Found (%): C, 31.08; H, 3.43; Br, 26.25; Cu, 10.72; N, 18.16. $C_{16}H_{20}Br_2CuN_8O_4$. Calculated (%): C, 31.41; H, 3.30; Br, 26.12; Cu, 10.38; N, 18.32.

IR, ν/cm^{-1}: 1554 ν(Cu—N) + δ(NCN); 200—300 (Cu—Br). ^1H NMR (D_2O), δ: 8.77 (br.s, 1 H, C(8)H); 3.96 (s, 3 H, N(7)CH_3); 3.30 (s, 3 H, N(1)CH_3); 2.24 (s, 3 H, N(3)CH_3). MS (ESI, 4.5 kV), m/z (I_{rel} (%)): 532.01 $[M - Br]^+$ (4), 451.14 $[M - 2\,Br]^{2+}$ (49). The mass spectra are indicative of the formation of the complex species $[Cu(caf)_2Br]^+$ and $[Cu(caf)_2]^+$: found m/z 532.01, calculated for $[Cu(caf)_2Br]^+$ 532.01; found m/z 451.14, calculated for $[Cu(caf)_2]^+$ 451.09; and also other fragments, including caffeine clusters.

Analytical studies were performed using equipment of the Shared Knowledge Center "Research Analytical Center of the National Research Center "Kurchatov Institute" — IREA". The powder X-ray diffraction analysis was performed using equipment of the Shared Facility Center for Physical Research Methods of the N. S. Kurnakov Institute of General and Inorganic Chemistry of the Russian Academy of Sciences within the framework of State assignments.

References

1. J. Ferlay, I. Soerjomataram, R. Dikshit, S. Eser, C. Mathers, M. Rebelo, D. M. Parkin, D. Forman, F. Bray, *Int. J. Cancer*, 2015, **136**, E359; DOI: 10.1002/ijc.29210.
2. U. Ndagi, N. Mhlongo, M. E. Soliman, *Drug Design Development Therapy*, 2017, **11**, 599.
3. D. R. Boer, A. Canals, M. Coll, *J. Chem. Soc.*, *Dalton Trans.*, 2009, **38**, 399; DOI: 10.1039/b809873p.
4. K. M. Deo, B. J. Pages, D. L. Ang, C. P. Gordon, J. R. Aldrich-Wright, *Int. J. Mol. Sci.*, 2016, **17**, 1818; DOI:10.3390/ijms17111818.
5. Y. Gou, J. Li, B. Fan, B. Xu, M. Zhou, F. Yang, *Eur. J. Med. Chem.*, 2017, **134**, 207; DOI: 10.1016/j.ejmech.2017.04.026.
6. F. Bacher, C. Wittmann, M. Nové, G. Spengler, M. A. Marć, E. A. Enyedy, D. Darvasiová, P. Rapta, T. Reinere, V. B. Arion, *J. Chem. Soc.*, *Dalton Trans.*, 2019, **48**, 10464; DOI: 10.1039/c9dt01238a.
7. L. Prashanth, K. K. Kattapagari, R. T. Chitturi, V. R. R. Baddam, L. K. Prasad, *J. Dr. NTR Univ. Health Sci.*, 2015, **4**, 75; DOI:10.4103/2277-8632.158577.
8. R. Tabti, N. Tounsi, C. Gaiddon, E. Bentouhami, L. Désaubry, *Med. Chem.*, 2017, **7**(5), 875; DOI: 10.4172/2161-0444.1000445.
9. M. L. Turski, D. J. Thiele, *J. Biol. Chem.*, 2009, **284**, 717.
10. R. Sanyal, S. K. Dash, S. Das, S. Chattopadhyay, S. Roy, D. Das, *J. Biolog. Inorg. Chem.*, 2014, **19**, 1099; DOI: 10.1007/s00775-014-1148-z.
11. N S. Rukk, L. G. Kuzmina, G. A. Davydova, G. A. Buzanov, V. M. Retivov, S. K. Belus, E. I. Kozhukhova, A. E. Barmashov, A. A. Khrulev, M. A. Simonova, V. N. Krasnoperova, *Mendeleev Commun.*, 2019, **29**, 640.
12. L. P. Vartanyan, M. B. Kolesova, G. F. Gornaeva, Yu. I. Pustovalov, *Psikhofarm. Biol. Narkol.* [*Psychopharm. Biol. Narcol.*], 2005, **5**, 1093 (in Russian).
13. M. Melnik, O. Sprusansky, P. Musil, *Adv. Biol. Chem.*, 2014, **4**, 274.

14. J. J. Hu, S.-Q. Bai, H. H. Yeh, D. J. Young, Y. Chi, T.S.A. Hor, *J. Chem. Soc.*, *Dalton Trans.*, 2011, **40**, 4402; DOI: 10.1039/c0dt01380c.
15. B. Ivanova, *Turk. J. Chem.*, 2007, **31**, 97.
16. H. A. Mohamed, B. M. R. Lake, T. Laing, M. Roger, R. M. Phillips, C. E. Willans, *J. Chem. Soc.*, *Dalton Trans.*, 2015, **44**, 7563; DOI: 10.1039/c4dt03679d.
17. B. Bertrand, L. Stefan, M. Pirrotta, D. Monchaud, E. Bodio, P. Richard, P. L. Gendre, E. Warmerdam, M. H. de Jager, G. M. M. Groothuis, M. Picquet, A. Casini, *Inorg. Chem.*, 2014, **53**, 2296; dx.doi.org/10.1021/ic403011h.
18. J.-J. Zhang, J. K. Muenzner, M. A. Abu el Maaty, B. Karge, R. Schobert, S. Wolfl, I. Ott, *J. Chem. Soc.*, *Dalton Trans.*, 2016, **45**, 13161; DOI: 10.1039/C6DT02025A.
19. G. Bandoli, M. C. Biagini, D. A. Clemente, G. Rizzardi, *Inorg. Chim. Acta*, 1976, **20**, 71.
20. N. S. Rukk, L. G. Kuzmina, R. S. Shamsiev, G. A. Davydova, E. A. Mironova, A. M. Ermakov, G. A. Buzanov, A. Yu. Skryabina, A. N. Streletskii, G. A. Vorob´eva, V. M. Retivov, P. A. Volkov, S. K. Belus, E. I. Kozhukhova, V. N. Krasnoperova, *Inorg. Chim. Acta*, 2019, **487**, 184; DOI: 10.1016/j.ica.2018.11.036.
21. T. Mossman, *J. Immunol. Methods*, 1983, **65**(1—2), 55.
22. R. A. Poltavtseva, Yu. A. Nikonova, I. I. Selezneva, A. K. Yaroslavtseva, V. N. Stepanenko, R. S. Esipov, S. V. Pavlovich, I. V. Klimantsev, N. V. Tyutyunnik, T. K. Grebennik, A. V. Nikolaeva, G. T. Sukhikh, *Bull. Exp. Biol. Med.*, 2014, **158**, 164; DOI: 10.1007/s10517-014-2714-7.
23. J. P. Henderson, J. Byun, M. V. Williams, M. L. McCormick, W. C. Parks, L. A. Ridnour, J. W. Heinecke, *Proc. Nat. Acad. Sci. USA*, 2001, **98**, 1631; DOI: 10.1073/pnas.041146998.
24. *Bruker, SAINT* (*Version 6.02a*), Bruker AXS Inc., Madison, Wisconsin, 2001, USA.
25. O. V. Dolomanov, L. J. Bourhis, R. J. Gildea, J. A. K. Hovard, H. Puschmann, *J. Appl. Crystallogr.*, 2009, **42**, 339.
26. *SHELXTL-Plus*, *Version 5.10*, Bruker AXS Inc., Madison, Wisconsin (USA), 1997.
27. C. F. Macrae, I. J. Bruno, J. A. Chisholm, P. R. Edgington, P. McCabe, E. Pidcock, L. Rodriguez-Monge, R. Taylor, J. van de Streek, P. A. Wood, *J. Appl. Crystallogr.*, 2008, **41**, 466; DOI: 10.1107/S0021889807067908.

Received October 10, 2019;
in revised form February 21, 2020;
accepted April 21, 2020